Cell

Structural Features of the GroEL-GroES Nano-Cage Required for Rapid Folding of Encapsulated Protein

Yun-Chi Tang,[1] Hung-Chun Chang,[1] Annette Roeben,[1] Dirk Wischnewski,[1] Nadine Wischnewski,[1] Michael J. Kerner,[1,2] F. Ulrich Hartl,[1,*] and Manajit Hayer-Hartl[1,*]
[1] Department of Cellular Biochemistry, Max Planck Institute of Biochemistry, Am Klopferspitz 18, D-82152 Martinsried, Germany
[2] Present address: Center for Biological Sequence Analysis, BioCentrum, Technical University of Denmark, Kemitorvet 208, DK-2800 Lyngby, Denmark.
*Contact: mhartl@biochem.mpg.de (M.H.-H.); uhartl@biochem.mpg.de (F.U.H.)
DOI 10.1016/j.cell.2006.04.027

SUMMARY

GroEL and GroES form a chaperonin nano-cage for proteins up to ~60 kDa to fold in isolation. Here we explored the structural features of the chaperonin cage critical for rapid folding of encapsulated substrates. Modulating the volume of the GroEL central cavity affected folding speed in accordance with confinement theory. Small proteins (~30 kDa) folded more rapidly as the size of the cage was gradually reduced to a point where restriction in space slowed folding dramatically. For larger proteins (~40–50 kDa), either expanding or reducing cage volume decelerated folding. Additionally, interactions with the C-terminal, mildly hydrophobic Gly-Gly-Met repeat sequences of GroEL protruding into the cavity, and repulsion effects from the negatively charged cavity wall were required for rapid folding of some proteins. We suggest that by combining these features, the chaperonin cage provides a physical environment optimized to catalyze the structural annealing of proteins with kinetically complex folding pathways.

INTRODUCTION

The GroEL/GroES chaperonin system of *Escherichia coli* fulfills an essential function in assisting the folding of cytosolic proteins (Fayet et al., 1989; Horwich et al., 1993; Ewalt et al., 1997). Approximately 250 different proteins interact with GroEL upon synthesis, of which ~85 are predicted to be obligate chaperonin substrates (Houry et al., 1999; Kerner et al., 2005). The basic mechanism of GroEL/GroES action involves encapsulation of a single molecule of nonnative protein in a cage-like structure, thereby allowing folding to occur unimpaired by aggregation (Mayhew et al., 1996; Weissman et al., 1996). However, recent experimental findings together with theoretical analyses suggest that the physical environment of the chaperonin cage, in addition to providing a sequestrated folding space, may profoundly affect the energy landscape and the kinetic trajectories along which folding proceeds (Brinker et al., 2001; Baumketner et al., 2003; Takagi et al., 2003; Jewett et al., 2004; Zhou, 2004). This offers the prospect of using the chaperonin system as an experimental tool to address a series of questions fundamental to our understanding of protein folding in general (Vendruscolo et al., 2003).

GroEL is a ~800 kDa cylindrical complex with ATPase activity, consisting of two heptameric rings of 57 kDa subunits, each forming a central cavity for the binding of nonnative protein. The subunits are divided into three domains (Braig et al., 1994; Saibil and Ranson, 2002). The apical domains, forming the ring opening, engage in multiple contacts with substrate protein via hydrophobic amino acid residues exposed toward the central cavity (Fenton et al., 1994). They are connected by a hinge-like intermediate domain to the equatorial ATPase domain. The cochaperone, GroES, is a dome-shaped heptameric ring of ~10 kDa subunits, which contact the apical GroEL domains via flexible loop sequences (Landry et al., 1993), thereby capping the opening of the GroEL cylinder (Xu et al., 1997).

The basic features of the GroEL mechanism have been revealed by a series of functional and structural studies (reviewed in Hartl and Hayer-Hartl, 2002; Fenton and Horwich, 2003). GroES cycles on and off GroEL in a manner allosterically regulated by the GroEL ATPase activity. Nonnative protein, exposing hydrophobic amino acid residues, binds with highest affinity to the nucleotide-free state of GroEL. Binding of ATP and of GroES then induces a structural conversion of the inner GroEL surface from hydrophobic to hydrophilic and generates an enclosed chamber with approximate dimensions of 80 Å in diameter and 85 Å in height (Xu et al., 1997). As a result, bound protein is transiently displaced into this cage and allowed to fold (Figure 1A) (Mayhew et al., 1996; Weissman et al., 1996). The enclosure time of ~10 s reflects the time required for the hydrolysis of the 7 ATP molecules in the

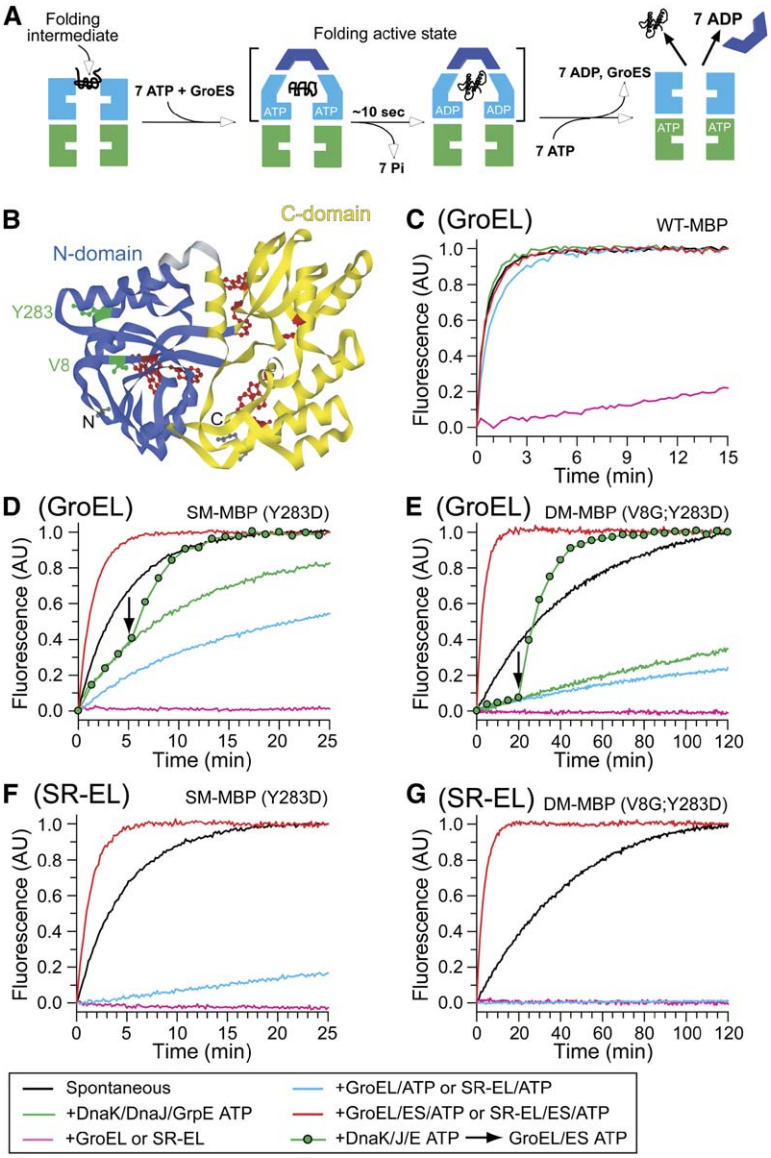

Figure 1. Effects of GroEL/GroES on Wild-Type and Mutant MBP Refolding

(A) Simplified model of the GroEL/GroES folding cycle. Note that multiple rounds of chaperonin action are generally required for completion of folding.

(B) Ribbon diagram of the structure of MBP (Spurlino et al., 1991; pdb 1OMP; DS ViewerPro), indicating the positions of mutated amino acids (green). The two discontinuous domains are shown in blue and yellow, respectively; the eight tryptophans are shown in red.

(C–G) Refolding of GuHCl-denatured MBP (25 μM) at 25°C upon 100-fold dilution into reactions containing either buffer A alone (spontaneous; black); buffer with 0.5 μM GroEL or 1.0 μM SR-EL (pink); 0.5 μM GroEL/5 mM ATP or 1.0 μM SR-EL/5 mM ATP (blue); 0.5 μM GroEL/1 μM GroES/5 mM ATP or 1.0 μM SR-EL/1 μM GroES/5 mM ATP (red); 1.25 μM DnaK/0.625 μM DnaJ/1.25 μM GrpE /5 mM ATP (green); or 1.25 μM DnaK/0.625 μM DnaJ/1.25 μM GrpE /5 mM ATP followed by addition of 0.5 μM GroEL/1 μM GroES/5 mM ATP (green circles) at the time indicated by the arrow. The maximum recovery of tryptophan fluorescence in the presence of GroEL/GroES/ATP was set to 1 (~100% of native MBP control).

GroES bound ring (the *cis*-ring) of GroEL. Following hydrolysis, GroES is triggered to dissociate by ATP binding to the *trans* GroEL ring. At this point, folded protein leaves GroEL, whereas incompletely folded states are rapidly recaptured for another folding attempt.

Obligate GroEL substrates are typically 30–50 kDa in size and display complex α/β or $\alpha+\beta$ domain topologies, with $(\beta\alpha)_8$ TIM barrel domains being overrepresented compared to the fold distribution of total cytosolic proteins (Kerner et al., 2005). These proteins appear to rely on GroEL to avoid or overcome kinetically trapped states whose accumulation would otherwise preclude folding at a biologically relevant time scale, thus favoring aggregation. As was shown for bacterial RuBisCo (50 kDa), a TIM barrel protein and model GroEL substrate, folding inside the cage occurs at a considerably faster rate than spontaneous folding, even when aggregation in free solution is avoided by adjusting protein concentrations to very low levels (Brinker et al., 2001). Theoretical analysis has attributed this rate enhancement to the spatial confinement experienced by the folding protein in the cage, which would entropically destabilize unfolded conformations and reduce the search time for the energy basin of the compact, native state (Baumketner et al., 2003; Takagi et al., 2003; Zhou, 2004).

Here, we performed a mutational analysis of the GroEL cavity to explore the structural features that play a critical role in accelerating folding. In support of geometric confinement as a major contributor, we show that reducing or increasing the volume of the chaperonin cage modulates folding speed systematically in a manner dependent on substrate size. In addition, we find that the flexible, mildly hydrophobic Gly-Gly-Met C-terminal repeats of GroEL and a number of conserved negative charges

exposed on the cavity wall are critical in facilitating rearrangement steps during folding of some proteins. These features in combination are required for optimal functionality of GroEL in vivo.

RESULTS

The Chaperonin Cage Can Accelerate Protein Folding More Than Ten-Fold

Proteins with an obligate GroEL dependence typically aggregate upon in vitro refolding (Kerner et al., 2005), and thus it is difficult to compare their spontaneous and chaperonin-assisted folding rates. To avoid this complication, we explored the suitability of maltose binding protein (MBP) as a model substrate based on previous reports that GroEL/GroES can increase the folding speed of a mutant form of MBP (Sparrer et al., 1997). MBP is a monomeric ~41 kDa periplasmic protein that folds robustly in the cytosol when expressed without its cleavable N-terminal export sequence. It is composed of two globular domains formed by discontinuous sequence elements consisting of secondary structural βαβ units with the binding site for maltose located in a cleft between the domains (Figure 1B) (Spurlino et al., 1991). Several slow-folding mutants of MBP are known, and we analyzed two of these, the single mutant Y283D (SM-MBP) and the double mutant V8G/Y283D (DM-MBP) (Chun et al., 1993; Wang et al., 1998). Mutations V8G and Y283D are located in close proximity in a strand and loop segment, respectively, of the N-domain (Figure 1B). Formation of native contacts within the N-domain is rate-limiting for folding and is slowed by these mutations (Chun et al., 1993). MBP possesses eight tryptophans distributed over both domains (Figure 1B). Their fluorescence signal is reduced 5-fold upon unfolding, and the recovery of fluorescence can be used as a measure of folding (Chun et al., 1993) both in the presence and absence of GroEL/GroES, which lack tryptophans.

Upon dilution from 6 M guanidine-HCl (GuHCl) at 25°C, wt-MBP refolded with an apparent rate of ~0.03 s^{-1} ($t_{1/2}$ ~25 s). SM-MBP and DM-MBP refolded to full yield but with ~7-fold ($t_{1/2}$ ~175 s) and ~75-fold ($t_{1/2}$ ~1900 s) slower rates, respectively (Figures 1C–1E and Table S1). In the absence of ATP, GroEL inhibited the spontaneous folding of all three proteins, indicating efficient recognition of unfolded MBP by chaperonin. In the presence of ATP, slow refolding was observed with SM-MBP and DM-MBP, whereas wt-MBP refolded with kinetics similar to spontaneous folding, suggesting that the mutant proteins bury hydrophobic residues more slowly, allowing efficient GroEL rebinding. Importantly, in the presence of GroES, the folding of SM-MBP was accelerated ~3-fold and that of DM-MBP ~13-fold compared to spontaneous folding (Figures 1C–1E and Table S1). In contrast to GroEL/GroES, the bacterial Hsp70 chaperone system, consisting of DnaK (Hsp70), DnaJ, GrpE, and ATP, strongly retarded the folding of SM-MBP and DM-MBP but maintained both proteins competent for accelerated folding by GroEL/GroES (Figures 1D and 1E). Very similar properties were recently described for several highly aggregation sensitive, authentic GroEL substrates (Kerner et al., 2005).

To confirm that the folding rates of MBP measured by tryptophan fluorescence reflected acquisition of the native state competent in binding maltose, we introduced a unique cysteine at position D95 in the N-domain and labeled it with the fluorophore IANBD. Binding of maltose to modified MBP results in a ~2- to 3-fold fluorescence increase at 538 nm (Marvin et al., 1997). Introduction of the D95C mutation slowed the spontaneous refolding of wild-type and mutant MBP, but very similar folding rates were determined by monitoring tryptophan or IANBD fluorescence (Table S1).

Temperature and denaturant-dependent unfolding experiments demonstrated that the native states of SM-MBP and DM-MBP were only moderately destabilized relative to wt-MBP and that the mutant proteins preserved cooperative unfolding behavior (Figure S1A and Table S1A) (Chun et al., 1993). Temperature-dependent unfolding was fully reversible, and folding rates and yields were essentially concentration-independent between 50 nM and 1 μM for wt-MBP (Ganesh et al., 2001) and for the two mutant proteins (Figures S1B–S1D), arguing against reversible aggregation as the cause of slow spontaneous folding of mutant MBP. Furthermore, chemical crosslinking by DTSSP (3,3′-dithiobis [sulfosuccinimidylpropionate]) between MBP monomers during refolding occurred only at protein concentrations above 1 μM (data not shown and Supplemental Experimental Procedures).

To demonstrate that encapsulation of mutant MBP in the GroEL-GroES cage is sufficient for accelerated folding, refolding experiments were carried out with the noncycling single-ring mutant of GroEL (SR-EL), which binds and encapsulates unfolded protein in a GroES- and ATP-dependent reaction but does not release GroES (Hayer-Hartl et al., 1996; Weissman et al., 1996). SR-EL/GroES in the presence of ATP fully reproduced the rate acceleration of SM-MBP and DM-MBP folding observed with the cycling GroEL/GroES system, while the rate of wt-MBP folding remained unchanged (Figures 1F and 1G and Table S1A). Thus, the physical environment of the GroEL-GroES cage is probably responsible for the observed increase in folding speed, as shown for RuBisCo (Brinker et al., 2001).

GroEL Mutants with Altered Cavity Size

The effect of topological confinement in the GroEL-GroES cage may contribute to accelerated folding by sterically blocking the formation of certain kinetically trapped conformers. To explore this possibility, we engineered a series of GroEL mutants with varying cavity size. The GroEL subunits contain flexible, C-terminal sequences of 13 residues, consisting of 4 Gly-Gly-Met (GGM) repeats and ending with an additional Met residue (Figure 2A). These $[GGM]_4M$ sequences protrude from the equatorial domains into the GroEL cavity but are not resolved in the crystal structure (Braig et al., 1994). Deletion or extension of these segments afforded the possibility to vary the size of the GroEL-GroES cage (Figure 2A). Taking the 7-fold

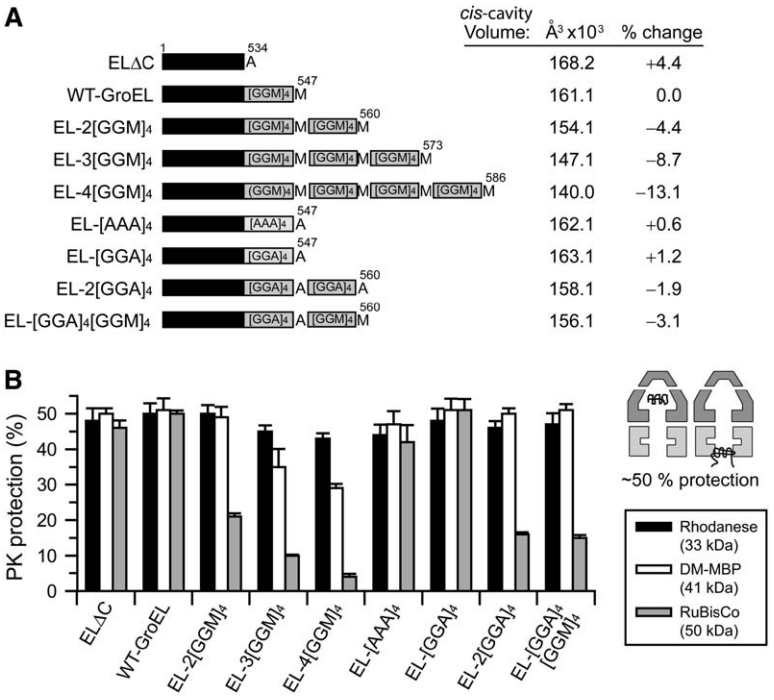

Figure 2. Properties of GroEL Cavity Size Mutants

(A) Schematic representation of a series of GroEL constructs with deletions, mutations, or extensions in the C-terminal $[GGM]_4$ repeat sequences. The *cis*-cavity volume of wild-type chaperonin was calculated as 161.1 Å^3 from the structure of the GroEL-GroES complex (Xu et al., 1997), taking into account that the N-terminal Met and C-terminal 23 amino acids of GroEL (~14,000 Å^3) were not resolved in the crystal structure. Volume changes resulting from modification of C-terminal segments were estimated based on the known volume of specific amino acid residues.

(B) Proteinase K (PK) protection of rhodanese, DM-MBP, or RuBisCo bound to wt-GroEL or GroEL mutants upon addition of GroES. GroEL-substrate complexes were incubated with PK in buffer A/4 mM AMP-PNP in the absence or presence of GroES at 25°C (see Experimental Procedures and Figure S3A). Protected substrate protein was quantified by immunoblotting and densitometry. Amounts in non-protease-treated reactions correspond to 100%. Error bars are a quantification of at least two independent experiments.

symmetry of the structure into account, we estimated that deletion of $[GGM]_4M$, resulting in ELΔC, would increase the volume capacity of GroEL for folding intermediates by ~4.4%. In contrast, duplication of the C-terminal segment (EL-2$[GGM]_4$) will reduce the volume by ~4.4% compared to wt-GroEL, and the mutants EL-3$[GGM]_4$ and EL-4$[GGM]_4$ are expected to have ~90% and 85% of wt-GroEL volume, respectively (Figure 2A). Additionally, by mutating $[GGM]_4$ to $[AAA]_4$, $[GGA]_4$, or $2[GGA]_4$, we changed the size of the cavity in small increments in a manner independent of the specific GGM sequence. These mutant chaperonins were generated both for GroEL and SR-EL. They bound unfolded protein with similar affinity as wt-GroEL, as evidenced by their ability to inhibit the spontaneous refolding of MBP in the absence of ATP (data not shown). Surface plasmon resonance experiments demonstrated efficient ATP-dependent GroES cycling and stable GroES binding in the presence of the nonhydrolysable ATP analog AMP-PNP (or ATP in case of non-cycling SR-EL) (data not shown).

To determine the functional volume capacity of the GroEL mutants, we measured the degree of protease protection conferred to GroEL bound substrate protein by GroES in the presence of AMP-PNP. As shown for rhodanese (33 kDa), DM-MBP (41 kDa), and bacterial RuBisCo (50 kDa), GroEL bound protein was rapidly degraded in the absence of GroES (Figure S2A). Addition of GroES to wt-GroEL resulted in ~50% protection of substrate, as expected due to the asymmetrical binding of GroES (Figure 2B) (Hayer-Hartl et al., 1996). While a similar degree of protection was observed with ELΔC, EL-$[AAA]_4$, and EL-$[GGA]_4$, the step-wise extension of the $[GGM]_4M$ segment resulted in a reduced capacity of protein encapsulation. This effect was most pronounced with the larger protein RuBisCo. For example, while EL-4$[GGM]_4$, having a ~13% reduced cavity volume, allowed efficient encapsulation of rhodanese, encapsulation of DM-MBP and RuBisCo was reduced by 40% and 90%, respectively (Figures 2B and S2A). Similar results were obtained with the cavity size mutants of SR-EL (data not shown).

Effects of GroEL Cavity Size on Folding

We next investigated how changing the size of the GroEL cavity affected the folding rates of proteins differing in molar mass, including mutant MBP (41 kDa) and the GroEL-dependent substrates rhodanese (33 kDa), MetF (33 kDa), and RuBisCo (50 kDa). Except for MBP, refolding conditions were nonpermissive, allowing essentially no refolding in the absence of chaperonin, due to aggregation.

Dependent on protein size, optimal folding rates were either observed with wt-GroEL or upon reduction of cage volume. Deletion of $[GGM]_4M$ (ELΔC), expanding the GroEL *cis* cavity by ~4.4%, generally reduced folding speed without changing the folding yields (Figures 3A–3F and S2B). Reducing wild-type cavity size by ~1.9, 3.1, and 4.4% in constructs EL-2$[GGA]_4$, EL-$[GGA]_4$ $[GGM]_4$, and EL-2$[GGM]_4$, respectively, resulted in a highly reproducible step-wise enhancement of folding rate for rhodanese and MetF (Figures 3A and 3B). This effect correlated well with the decrease in available cage volume of the GroEL mutants. It was independent of the hydrophobic Met residues in the C-terminal extensions and was therefore attributed to spatial confinement rather than to specific interactions with the extended GroEL sequences. Further reduction of cavity size (EL-3$[GGM]_4$) reversed the rate acceleration without affecting the folding yield. Finally, very

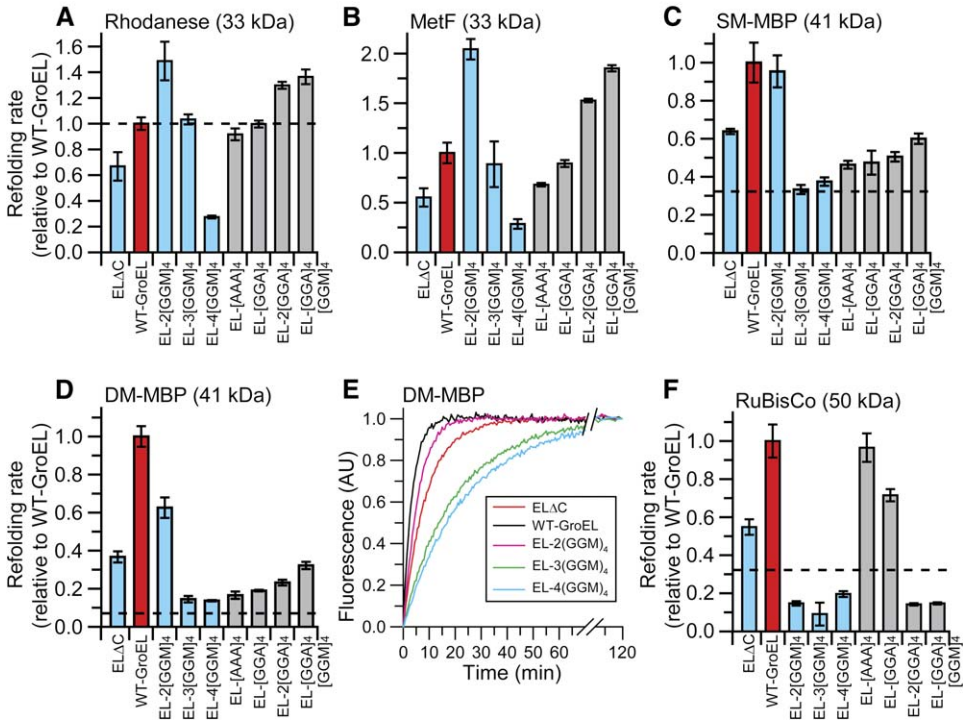

Figure 3. Effect of GroEL Cavity Size on Folding Rates

GroEL/GroES assisted refolding of rhodanese (A), MetF (B), SM-MBP (C), DM-MBP (D and E), and RuBisCo (F) at 25°C with the GroEL mutants indicated (see Experimental Procedures). Blue bars, cavity size mutants (decreasing cavity size from left to right); light gray bars, mutants with reduced hydrophobic character of the C-terminal repeat sequences. The refolding yield obtained with wt-GroEL (red bar) was set to 1. The dashed line represents the rate of spontaneous folding (not known for MetF). Representative tryptophan fluorescence folding traces for DM-MBP are shown in (E). Standard deviations of at least three independent experiments are shown.

slow folding below the spontaneous rate (dashed line) was observed with EL-4[GGM]$_4$ (Figures 3A and 3B), accompanied by a 40%–70% reduction in folding yield (Figure S2B). Because encapsulation of rhodanese and MetF by GroES was still fully efficient (Figure 2B), this indicates that space restriction limited critical rearrangement steps during folding. These effects were reproduced upon single-round encapsulation of the proteins in SR-4[GGM]$_4$ (data not shown).

In contrast to rhodanese and MetF, reducing cavity size did not accelerate folding for the larger protein MBP. While EL-2[GGM]$_4$ still supported folding of SM-MBP at the rate seen with wt-GroEL, the folding speed of DM-MBP was ~40% reduced, suggesting that the folding pathways of the mutant proteins differ (Figures 3C–3E). Further reduction in cavity size (EL-3[GGM]$_4$) slowed the folding of both proteins without reducing the folding yield (Figures 3C, 3D, and S2B), although encapsulation by GroES was still ~70% efficient (Figure 2B and data not shown). These results were confirmed with the cavity size mutants of SR-EL (data not shown). A sequence-specific effect of [GGM]$_4$M on folding will be discussed below.

Consistent with its larger size, the folding of RuBisCo was even more strongly affected by decreasing the volume of the chaperonin cage (Figure 3F). This effect was independent of the specific sequence of the C-terminal extension because both EL-2[GGA]$_4$ and EL-2[GGM]$_4$ equally slowed RuBisCo folding to below its spontaneous rate (Figure 3F) without affecting the yield (Figure S2B). However, the folding yield was reduced by ~50% with EL-3[GGM]$_4$ and by ~95% with EL-4[GGM]$_4$, correlating with the loss of encapsulation (Figure 2B).

Fluorescence anisotropy measurements using the D95C variants of mutant MBP labeled with Alexa 488 confirmed that reducing cavity size restricted the mobility of enclosed protein. These experiments were performed with the noncycling SR-EL cavity size mutants. When bound to the apical domains of SR-EL, the anisotropy value of the unfolded protein was high, reflecting the low rotational dynamics of the large SR-EL-substrate complex (Figures 4A and 4B). Upon GroES binding triggered by ATP addition, a rapid drop in anisotropy occurred, indicating increased dynamics resulting from displacement of the bound protein into the cage (Rye et al., 1997). For SM-MBP in SR-EL or SR-2[GGM]$_4$, this step was followed by a time-dependent increase in mobility occurring with kinetics corresponding to folding, as measured by tryptophan fluorescence (Figure 4A and data not shown). In contrast, the folding protein was increasingly restricted in mobility in SR-3[GGM]$_4$ and SR-4[GGM]$_4$ (Figure 4A).

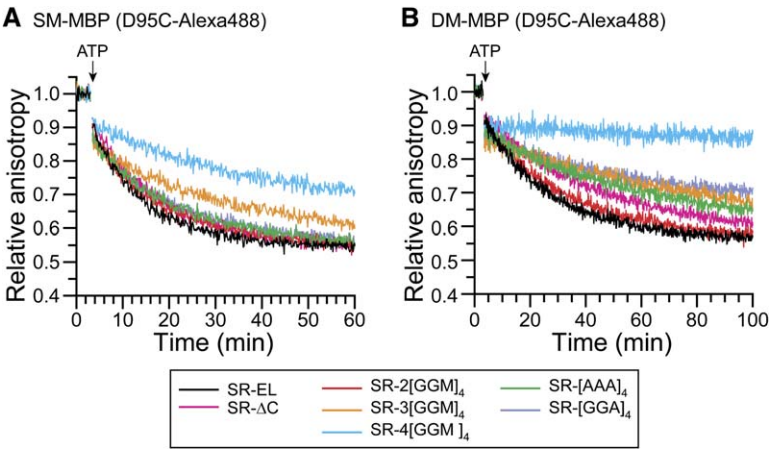

Figure 4. Restriction in Substrate Protein Mobility upon Encapsulation in SR-EL and in SR-EL with Mutated C-Terminal Sequences

Kinetics of steady-state fluorescence anisotropy of SM-MBP (A) and DM-MBP (B) upon encapsulation by GroES in the SR-EL cavity size mutants indicated. D95C versions of MBP were labeled with Alexa 488 (see Experimental Procedures). GroES binding was initiated by addition of ATP (arrow). Note that removal of nonencapsulated DM-MBP by proteinase K in the reaction with SR-4[GGM]$_4$ in (B) had only a small effect on anisotropy, indicating that largely encapsulated protein was measured.

DM-MBP generally experienced a more pronounced restriction in mobility (Figure 4B), suggesting that this protein populates more extended folding intermediates.

These results are consistent with theoretical simulations of the effects of steric confinement on protein folding (Baumketner et al., 2003; Takagi et al., 2003; Zhou, 2004), which predict that proteins will experience a rate acceleration of folding with increasing confinement up to a point where further restriction in space would limit necessary reconfiguration steps.

Function of the Mildly Hydrophobic GGM Repeats in Folding

The flexible, mildly hydrophobic GGM repeats of GroEL are highly conserved among GroEL homologs from different species (Brocchieri and Karlin, 2000). GroEL lacking this sequence was found to support the growth of *E. coli* but, in contrast to wt-GroEL, was unable to suppress temperature sensitive mutations in various proteins (McLennan et al., 1993). We found that changing [GGM]$_4$M to [AAA]$_4$A or [GGA]$_4$A decelerated the folding of mutant MBP to a greater extent than deleting [GGM]$_4$M altogether (Figures 3C and 3D). Anisotropy measurements revealed that, contrary to expectations, increasing cavity size by deleting [GGM]$_4$M (SRΔC) did not increase protein mobility during folding (Figures 4A and 4B). Moreover, replacement of [GGM]$_4$M by [AAA]$_4$A caused a substantial restriction in mobility of the folding protein, an effect that was again most pronounced with DM-MBP and was not seen with wt-MBP (Figure 4B and data not shown). Notably, these mutations had only a small effect on the folding of rhodanese, MetF, and RuBisCo (Figures 3A, 3B, and 3F). Similarly, mutants EL-2[GGA]$_4$ and EL-[GGA]$_4$[GGM]$_4$ were less effective than EL-2[GGM]$_4$ in the folding of mutant MBP (Figures 3C and 3D). These results argue for a specific role of [GGM]$_4$ in facilitating the rearrangement of certain folding intermediates by providing a mildly hydrophobic, interactive surface. This function may be particularly important for proteins which have acquired mutations that result in highly energetically frustrated folding pathways, such as the mutant versions of MBP.

Role of Negative Charge Clusters on the GroEL Cavity Wall

The wall of the GroEL *cis* cavity has a net charge of −42 (189 negatively and 147 positively charged amino acid residues). A number of negative charges (residues E252, D253, E255, D359, D361, and E363), all in the apical domain, cluster in two circular layers (Figure 5A). Most of these residues (E252, D253, E255, E363) are highly conserved among GroEL homologs, although they have no apparent role in the basic GroEL functions of substrate and GroES binding (Brocchieri and Karlin, 2000; Stan et al., 2003). To explore their possible significance in promoting folding, we replaced individual or multiple residues by either asparagine or glutamine (neutral) or lysine (positive) in SR-EL. As a consequence of the 7-fold symmetry of GroEL, these mutations dramatically change the electrostatic character of the cavity wall (Figure 5A). The mutant proteins were efficiently overexpressed and purified in soluble form. All the SR-EL charge mutants bound GroES stably in the presence of ATP, reflecting the inability of SR-EL to cycle GroES (data not shown). Binding of GroES to preformed complexes of mutant SR-EL and unfolded DM-MBP resulted in 90%–100% protease protection (Figures 5B and S3A). In contrast, several of the SR-EL charge mutants had a 40%–50% reduced capacity to support RuBisCo encapsulation, suggesting an interference with the compaction of the molecule normally occurring upon its displacement into the cage by GroES (Lin and Rye, 2004). A ~75% reduced encapsulation efficiency was observed with mutation D253K (Figures 5B and S3A). This mutant was not analyzed further with regard to RuBisCo folding.

The charge mutations were without effect on the rate or yield of wt-MBP folding but moderately reduced the folding speed of SM-MBP and markedly decelerated DM-MBP folding (Figures 6A–6C and S3B). Changing single or multiple negative charges to neutral residues slowed DM-MBP folding by 30 to 80%, with multiple mutations generally having a more severe effect (Figure 6C). The effects of replacing negative with positively charged residues varied considerably dependent on the specific

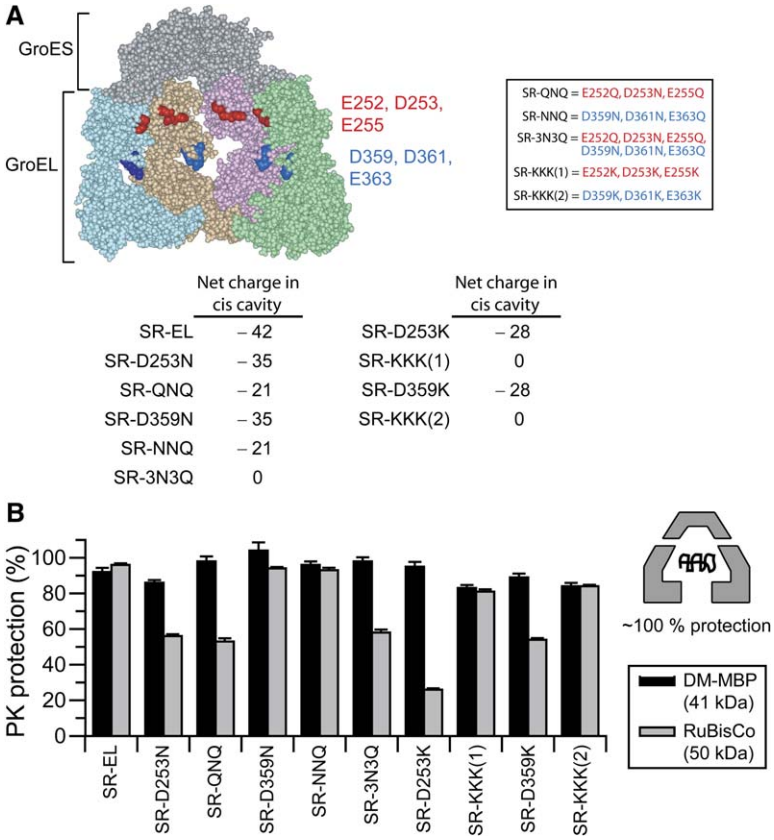

Figure 5. Properties of GroEL Cavity-Charge Mutants

(A) Space-filling model of GroEL/GroES-$(ADP)_7$ complex (Xu et al., 1997; pdb 1AON, DS ViewerPro) offering a view into the *cis*-cavity with four subunits of GroEL and GroES shown. Clusters of negatively charged residues exposed toward the *cis*-cavity are highlighted in red (E252, D253, E255) and blue (D359, D361, E363). The net charge of the *cis*-cavity wall formed by 7 GroEL subunits is indicated for the different mutants.

(B) PK protection of DM-MBP and RuBisCo in complexes with the various mutant forms of SR-EL and GroES. PK treatment was performed as in Figure 2B (also see Figure S4A). Amounts of DM-MBP and RuBisCo in nonprotease treated reactions correspond to 100%. Error bars are a quantification of at least two independent experiments.

protein tested. For example, the single-charge reversal of SR-D359K, while strongly decelerating the folding of DM-MBP, caused a moderate acceleration of rhodanese folding and was without effect on the folding rate of RuBisCo (Figure 6D). In the case of RuBisCo, some of the charge mutants strongly diminished the folding yield. An interesting example is SR-NNQ, which caused an 80% reduction in yield (Figure S3B), although the protein was efficiently encapsulated by GroES (Figure 5B). However, the subpopulation of molecules that reached native state did so at almost normal apparent rate (Figure 6D). This indicated that a large fraction of RuBisCo was trapped inside the SR-EL-GroES cage in a nonnative state. A virtually complete folding arrest of encapsulated RuBisCo was observed with SR-KKK(2), containing positive charges at positions D359, D361, and E363. Indeed, upon dissociation of GroES at low temperature in the presence of EDTA, most of the RuBisCo was released from the cavity in a PK-sensitive, nonnative state. In contrast, PK-resistant folded protein was detected when the same experiment was carried out with wild-type SR-EL (data not shown). The complete removal of cavity net charge in SR-KKK(2) also strongly decelerated the folding of DM-MBP but caused a moderate increase in folding speed for rhodanese (Figures 6C and 6D). It is noteworthy in this context that wt-MBP, mutant MBP, and RuBisCo have a negative net charge of −8, −9, and −11, respectively, whereas rhodanese, the protein least affected by the charge mutations, has a net charge of only −1 (Table S2).

Reducing the negative net charge of the cavity wall strongly impaired the mobility of MBP in the chaperonin cage. This effect was already apparent with the D95C version of wt-MBP (Figure S4A). The protein interacted substantially with the less negatively charged cavity wall, both during folding and after reaching native state. However, mobility was increasingly more restricted with the slower folding SM-MBP and DM-MBP (Figures S4B and S4C). Mutants which caused complete loss of cavity-wall net charge, such as SR-3N3Q and SR-KKK(2) (Figure 5A), significantly slowed the rapid mobilization of SM-MBP and DM-MBP normally occurring immediately upon GroES binding (Figures S4B and S4C). This suggests that the nonnative states of these proteins interact with the cavity wall immediately after release from the apical GroEL domains, presumably resulting in delayed burial of hydrophobic residues.

These findings indicate that the charge properties of the GroEL cavity wall are of profound significance in the ability of the chaperonin to promote the folding of certain substrate proteins. While the charge effects on specific proteins may vary, the overall negative surface charge of the cavity wall of the apical domains appears to provide a noninteractive surface optimized to accomplish the efficient folding of many different proteins.

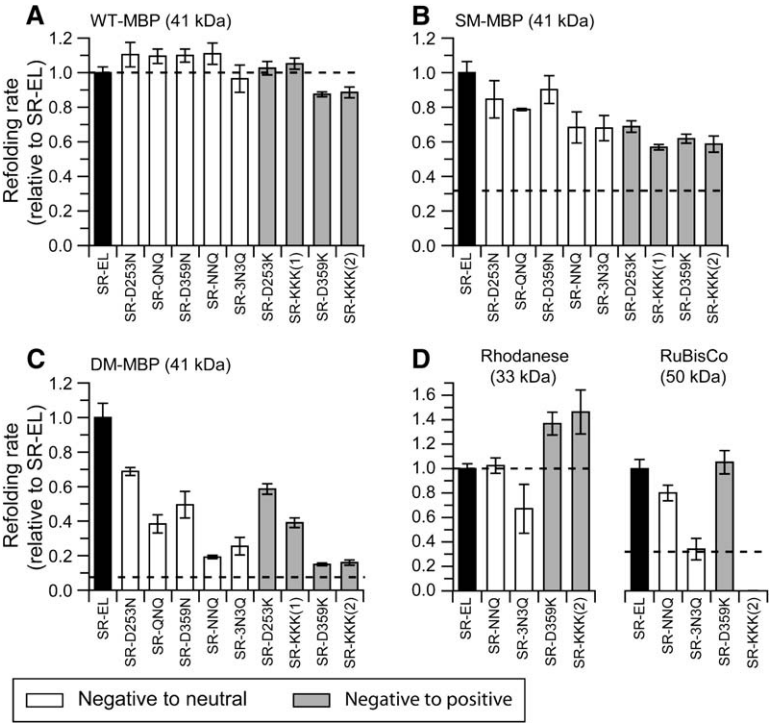

Figure 6. Effect of GroEL Cavity Charge on Folding Rates

Refolding of wt-MBP (A), SM-MBP (B), DM-MBP (C), rhodanese and RuBisCo (D) with the indicated SR-EL charge mutants and GroES was analyzed in buffer B/5 mM ATP at 25°C as described in Experimental Procedures. White bars indicate amino acid changes from negative to neutral, and light gray bars indicate changes from negative to positive. The refolding rate obtained with SR-EL was set to 1 (black bar). Dashed line represents the rate of spontaneous folding for the respective proteins. Standard deviations of at least three independent experiments are shown.

Significance of Accelerated Folding by GroEL/GroES In Vivo

The requirement of GroEL/GroES for efficient protein folding in vivo is well established, but it is unclear whether the capacity of the chaperonin to accelerate folding is biologically relevant. We addressed this question using MBP and MetF as model substrates. Overexpression of wt-MBP from an arabinose-controlled expression plasmid in *E. coli* resulted in the production of fully soluble protein. In contrast, expression of SM-MBP, DM-MBP, and MetF produced largely insoluble protein (Figure 7A). Additional overexpression of GroEL/GroES, but not of GroEL alone, dramatically reduced the formation of aggregates and allowed the production of soluble protein (Figures 7B and 7C). Overexpression of ELΔC suppressed the aggregation of SM-MBP, DM-MBP, and MetF only partially (Figure 7D), consistent with the reduced folding rates observed with ELΔC in vitro (Figures 3B–3D). Expression of the GroEL variant with reduced cavity size, EL-2[GGM]$_4$, resulted in a similar effect in the case of mutant MBP but allowed the production of soluble MetF with close to 100% yield (Figure 7E). This enhancement of solubility corresponds with the accelerated folding of MetF by EL-2[GGM]$_4$ observed in vitro (Figure 3B). As expected, EL-4[GGM]$_4$ was unable to support the folding of mutant MBP or MetF (Figure 7F). Changing the repeat motif from [GGM]$_4$M to [GGA]$_4$A failed to produce significant amounts of native mutant MBP but partially suppressed the aggregation of MetF (Figure 7G), confirming the sequence-specific contribution of [GGM]$_4$M to mutant MBP folding (Figures 3C and 3D). Similarly, the charge mutants EL-NNQ, EL-3N3Q, and EL-KKK(2) were only partially efficient in MetF and SM-MBP folding and strongly reduced the amount of soluble mutant MBP (Figures 7H–7J), again consistent with the observations in vitro (Figures 6B and 6C). Collectively, these results demonstrate the biological relevance of accelerated folding achieved by the chaperonin system. Reducing the ability of GroEL to accelerate folding diminishes its capacity to handle recalcitrant proteins such as the mutant versions of MBP. On the other hand, decreasing the size of the GroEL cavity is beneficial for the folding of the smaller protein, MetF.

DISCUSSION

GroEL/GroES—More Than an Infinite Dilution Box

The GroEL/GroES nano-cage allows a single protein molecule to fold in isolation. This reaction has been compared to spontaneous folding at infinite dilution. However, recent experimental and theoretical studies indicated that the physical environment of the chaperonin cage can alter the folding energy landscape, resulting in accelerated folding for some proteins. By performing an extensive mutational analysis of GroEL, we have identified three structural features of the chaperonin cage as major contributors to this capacity: (1) geometric confinement exerted on the folding protein inside the limited volume of the cage; (2) a mildly hydrophobic, interactive surface at the bottom of the cage; and (3) clusters of negatively charged amino acid residues exposed on the cavity wall. We suggest that these features in combination provide a physical environment that has been optimized in evolution to

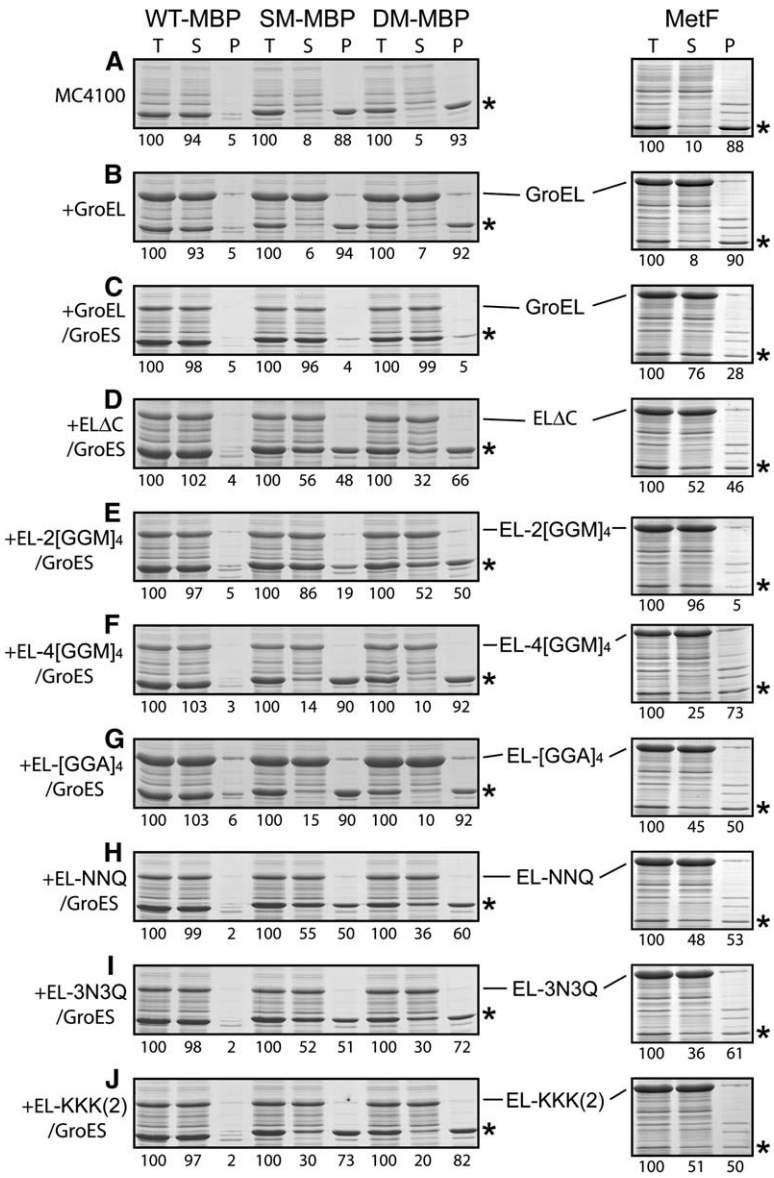

Figure 7. Effect of wt-GroEL and GroEL Mutants on Folding In Vivo

wt-MBP, SM-MBP, DM-MBP, or MetF were overexpressed in *E. coli* cells of strain MC4100C either without (A) or with additional overexpression of GroES and the GroEL mutants indicated (C–J) (see Experimental Procedures). GroES expression was omitted in (B). Total (T), supernatant (S), and pellet (P) fractions were analyzed by SDS-PAGE and Coomassie staining. Amounts of MBP or MetF protein in S and P fractions, determined by densitometry, are given in % with total protein (T) set to 100%. The asterisk indicates the position of MBP or MetF.

catalyze the structural annealing of proteins with kinetically complex folding pathways. Thus, the chaperonin system and its mutant versions may prove as useful tools in understanding how proteins navigate their energy landscape of folding.

Effect of Spatial Confinement on Folding Rate

In the crystal structure, the GroEL-GroES cage has a total volume of ~175,000 Å^3, in principle large enough to accommodate proteins of >70 kDa (Xu et al., 1997). However, the functionally relevant volume is smaller due to the C-terminal 23 amino acids of the GroEL subunits, which protrude into the cavity but are not resolved in the structure. Because of their flexible character, these segments are likely to occupy more than their nominal volume of ~14,000 Å^3 per GroEL ring. Moreover, since the geometry of the cage resembles a truncated cone, part of the volume may be unavailable to certain substrate proteins. Consistent with these considerations, most GroEL-dependent proteins are smaller than 50 kDa (Kerner et al., 2005), and the 56 kDa phage T4 capsid protein, Gp23, requires an enlarged phage-encoded version of GroES (Gp31) for encapsulation (Hunt et al., 1997; Bakkes et al., 2005). It follows that a typical GroEL substrate would undergo considerable compaction upon displacement into the cage from a loosely packed bound state (Horst et al., 2005). This step is mediated by ATP and GroES binding, which drive large allosteric domain movements in GroEL (Figure 1A). The geometric confinement exerted by the cage would result in a destabilization of unfolded conformers relative to bulk solution and in the preferential population of compact intermediates, thus potentially

smoothing rugged folding energy landscapes and enhancing the folding rate (Brinker et al., 2001; Baumketner et al., 2003; Takagi et al., 2003; Zhou, 2004). Because the entropic penalty for establishing long-range interactions is large, the acceleration of folding is predicted to be more pronounced for proteins with a high proportion of long-range tertiary contacts (Takagi et al., 2003) such as the GroEL-dependent proteins with complex α/β or $\alpha+\beta$ domain topologies (Kerner et al., 2005).

We have performed the first systematic test of these ideas by gradually reducing or increasing the volume of the chaperonin cage. The results of these experiments are remarkably consistent with prediction. Relatively small proteins such as rhodanese and MetF (33 kDa) experienced a rate acceleration of folding upon reducing cage size to a point where further restriction in space slowed folding dramatically. For MBP (41 kDa) and RuBisCo (50 kDa), on the other hand, either reducing or increasing cage volume decelerated folding, indicating that wt-GroEL provides an optimal level of spatial confinement for these proteins. The optimum for productive confinement proved to be remarkably narrow, with as little as 2%–5% change in cage volume affecting folding rates by 2-fold or more. Theory predicts a maximum effect of confinement on folding rate if the rate-limiting transition state intermediates of a given protein are relatively similar in compactness to the native state. On the other hand, ''over-confinement'' may stabilize misfolded states that require substantial expansion in order to return to a productive folding trajectory. Taking the geometries of cage and substrate proteins into consideration, the extent of conformational movement possible during folding is indeed very limited. For rhodanese, MetF, and MBP, the longest axes of the native proteins are between 60–73 Å, compared to 85 Å as the longest dimension of the cage (Table S2). Remarkably, in the case of RuBisCo, the long axis of the native monomer is 95 Å, suggesting either that the GroEL-GroES complex is conformationally plastic or the product of RuBisCo folding is a compressed monomer. The latter possibility would be consistent with recent FRET measurements for this protein when enclosed in the GroEL-GroES cage (Lin and Rye, 2004).

Physical Properties of the GroEL Cavity Wall

In theoretical models of confinement, proteins are generally assumed to be enclosed in a volume limited by an inert wall. Our mutational analysis demonstrates that polar and hydrophobic wall properties of the chaperonin cage, acting in conjunction with geometric confinement, contribute critically to the ability of the system to accelerate folding. The cavity wall has a net charge of -42 with several negative charge clusters at the level of the apical GroEL domains (Figure 5A). This would result in electrostatic repulsion effects, given that most GroEL substrates have a negative net charge (Kerner et al., 2005). Charged residues on the inner surface of the GroES lid may also contribute to this effect (Hunt et al., 1997; Wang et al., 2002). In contrast, the flexible GGM repeat sequences, emanating from the equatorial domains of GroEL, provide an interactive surface of mildly hydrophobic character. Interestingly, molecular dynamics simulations of the folding of a highly energetically frustrated protein inside the chaperonin cage suggested that a moderately hydrophobic wall would accelerate folding substantially (Jewett et al., 2004). The GGM repeats may fulfill such a role, perhaps by intercalating between hydrophobic regions of folding intermediates, thereby preventing the formation of kinetically stable, misfolded states.

Our results support a model in which the bimodal character of the cavity wall facilitates the reconfiguration of folding intermediates within the confined cage. Notably, the resulting annealing mechanism is independent of repeated cycles of active GroES and ATP-dependent unfolding, in contrast to the ''iterative annealing'' model (Thirumalai and Lorimer, 2001). Instead, ''cage-mediated annealing'' would achieve a smoothing of the folding energy landscape in a single encapsulation cycle by sequestrating the protein in a confined space with an optimized mixture of hydrophobic and electrostatic wall properties. Consistent with this proposal, changes in these properties had the most pronounced effect on the folding of DM-MBP and RuBisCo, those proteins in the test set which experienced the highest enhancement in folding rate by GroEL.

Biological Relevance of Cage-Mediated Annealing

Based on our recent analysis of the GroEL substrate proteome, ~85 *E. coli* cytoplasmic proteins are predicted to be strictly dependent on GroEL/GroES for folding, including 13 proteins with essential functions (Kerner et al., 2005). It would appear that the chaperonin cage has been optimized to accomplish the folding of these proteins at a biologically relevant time scale. As noted previously, the properties of the cage must therefore represent an evolutionary compromise to support a variety of folding pathways (Wang et al., 2002), and this would explain why mutating certain features may improve the folding of a specific protein while potentially being detrimental to the folding of others. However, significant structural deviations may be tolerated when additional specialized forms of GroEL are expressed to allow adaptation of an organism to specific growth conditions. Interestingly, Mycobacteria express two forms of GroEL, of which GroEL1 lacks the C-terminal GGM repeat and instead has an 18 amino acid, histidine-rich sequence. This C-terminal sequence appears to be critical for GroEL1 to support the folding of proteins required for bacterial biofilm formation (Ojha et al., 2005).

An additional important role of cage-mediated annealing is to preserve the foldability of a protein despite the presence of mutations, as shown for mutant MBP. This capacity would explain the recent finding that overproduction of GroEL/GroES reduces the phenotypic penetrance of deleterious mutations in bacterial cell lineages (Maisnier-Patin et al., 2005) in a manner comparable to the conformational buffering effects proposed for other chaperone systems (Rutherford and Lindquist, 1998).

EXPERIMENTAL PROCEDURES

Strains and Plasmids

GroEL mutants were constructed in a pCH vector backbone (Chang et al., 2005) inserted via the *Nde*I and *Nhe*I sites. Synthetic oligonucleotides encoding wild-type or mutant C-terminal extensions of GroEL were introduced into the pCH-ELΔC or SR-ELΔC plasmid between the *Nhe*I and *Hind*III sites. The SR-EL charge mutants (SR-QNQ, SR-NNQ, SR-3N3Q, SR-KKK(1), SR-KKK(2), SR-D253N, SR-D253K, SR-D359N, and SR-D359K) and MBP mutants (SM-MBP (Y283D), DM-MBP (V8G,Y283D), wt-MBP (D95C), SM-MBP (D95C), DM-MBP (D95C)) were generated by site-directed mutagenesis. wt and mutant MBP were expressed in vivo using the arabinose promoter controlled vector pBAD18 (Guzman et al., 1995).

Proteins

Chaperone proteins DnaK, DnaJ, GrpE, GroEL, SR-EL, GroES, GroEL mutants, and SR-EL mutants were purified as described (Hayer-Hartl et al., 1996; Kerner et al., 2005). MBP and MBP mutants were purified using an amylose affinity column (New England Biolab). Bovine mitochondrial rhodanese (Sigma), MetF (Kerner et al., 2005), and RuBisCo from R. rubrum (Brinker et al., 2001) were purified as described. Protein concentrations were determined spectrophotometrically at 280 nm.

Refolding Assays

wt-MBP and mutants (25 μM) were denatured in 20 mM Tris, pH 7.5, 20 mM KCl, 6 M GuHCl and refolded upon 100-fold dilution into high-salt buffer A (20 mM Tris, pH 7.5, 200 mM KCl, 5 mM $Mg(OAc)_2$) or low-salt buffer B (20 mM Tris, pH 7.5, 20 mM KCl, 5 mM $Mg(OAc)_2$) in the absence or presence of chaperones. GroEL/GroES-assisted refolding was initiated at 25°C by the addition of 5 mM ATP. Intrinsic tryptophan fluorescence was monitored on a Fluorolog 3 Spectrofluorometer (Spex) with an excitation wavelength of 295 nm (slit width 2 nm) and an emission wavelength of 345 nm (slit width 5 nm). Refolding of MetF, rhodanese, and RuBisCo was performed as described (Hayer-Hartl et al., 1996; Brinker et al., 2001; Kerner et al., 2005) (see Supplemental Experimental Procedures).

Fluorescence Assay of Maltose Binding by MBP

MBP D95C mutants (50 μM) (Marvin et al., 1997) were labeled in buffer C (100 mM HEPES, pH 7.8, 1 mM TCEP, 2 mM EDTA) for 4 hr on ice in the presence of a 20-fold excess of the fluorophore IANBD (*N*-((2-(iodoacetoxy) ethyl)-*N*-methyl) amino-7-nitrobenz-2-oxa-1, 3-diazole ester, Molecular Probes, Inc.). Unbound fluorophore was removed using micro Bio-Gel P6 columns (BIO-RAD) equilibrated in buffer B. The coupling efficiency measured by the absorption of MBP (ε_{280} = 69 $mM^{-1}cm^{-1}$), and IANBD (ε_{472} = 23 $mM^{-1}cm^{-1}$) was >90%. IANBD fluorescence was monitored at 538 nm (slit width 8 nm) with an excitation wavelength at 470 nm (slit width 2 nm) at 25°C.

Fluorescence Anisotropy

MBP D95C mutants (50 μM) (Marvin et al., 1997) were labeled in buffer C for 12 hr on ice with a 2.5-fold excess of Alexa Fluor 488 C_5 maleimide (Molecular Probes). Unbound fluorophore was removed as above. The coupling efficiency measured by the absorption of MBP (ε_{280} = 69 $mM^{-1}cm^{-1}$) and Alexa 488 C_5 maleimide (ε_{493} = 72 $mM^{-1}cm^{-1}$) was >90%. Anisotropy was monitored at the emission wavelength of 518 nm (slit width 7 nm) with an excitation wavelength at 495 nm (slit width 5 nm) at 25°C using a LS50 spectrophotometer (Perkin-Elmer).

Proteinase K Protection of GroEL-GroES-Substrate Complexes

Rhodanese, DM-MBP, or RuBisCo (25 μM each) was denatured as described above and diluted 100-fold into buffer A or B in the presence of a 2- or 4-fold molar excess of GroEL or SR-EL, respectively, at 25°C. Treatment with proteinase K (2 μg/ml) was followed for 0–20 min (Hayer-Hartl et al., 1996). Protease protection of substrate protein was determined by immunoblotting.

Solubility of MBP In Vivo

E. coli MC4100 strain containing the plasmid pOFXtac-SL2 (Agashe et al., 2004), expressing GroEL/GroES or EL mutants/GroES, was transformed with the arabinose-controlled expression plasmid for MBP or MetF. Cells were grown in LB medium at 37°C to an OD_{600} = 0.8, and chaperonins were induced with 0.1 mM IPTG for 1 hr before induction of substrate protein with 0.2% arabinose for 1 hr. Spheroplasts were prepared and fractionated as described (Chang et al., 2005).

Supplemental Data

Supplemental Data include four figures, two tables, and Experimental Procedures and can be found with this article online at http://www.cell.com/cgi/content/full/125/5/903/DC1/.

ACKNOWLEDGMENTS

We thank L. Randall for providing E. coli strains *malE* (HB1045) and *malE Y283D* (HB1204), A. Minton for discussions, and S. Broadley and K. Chakraborty for critically reading the manuscript. This work was supported by the Deutsche Forschungsgemeinschaft and the Ernst Jung Foundation.

Received: February 15, 2006
Revised: March 29, 2006
Accepted: April 4, 2006
Published: June 1, 2006

REFERENCES

Agashe, V.R., Guha, S., Chang, H.C., Genevaux, P., Hayer-Hartl, M., Stemp, M., Georgopoulos, C., Hartl, F.U., and Barral, J.M. (2004). Function of trigger factor and DnaK in multidomain protein folding: Increase in yield at the expense of folding speed. Cell *117*, 199–209.

Bakkes, P.J., Faber, B.W., van Heerikhuizen, H., and van der Vies, S.M. (2005). The T4-encoded cochaperonin, gp31, has unique properties that explain its requirement for the folding of the T4 major capsid protein. Proc. Natl. Acad. Sci. USA *102*, 8144–8149.

Baumketner, A., Jewett, A., and Shea, J.E. (2003). Effects of confinement in chaperonin assisted protein folding: Rate enhancement by decreasing the roughness of the folding energy landscape. J. Mol. Biol. *332*, 701–713.

Braig, K., Otwinowski, Z., Hegde, R., Boisvert, D.C., Joachimiak, A., Horwich, A.L., and Sigler, P.B. (1994). The crystal structure of the bacterial chaperonin GroEL at 2.8 A. Nature *371*, 578–586.

Brinker, A., Pfeifer, G., Kerner, M.J., Naylor, D.J., Hartl, F.U., and Hayer-Hartl, M. (2001). Dual function of protein confinement in chaperonin-assisted protein folding. Cell *107*, 223–233.

Brocchieri, L., and Karlin, S. (2000). Conservation among HSP60 sequences in relation to structure, function, and evolution. Prot. Sci. *9*, 476–486.

Chang, H.C., Kaiser, C.M., Hartl, F.U., and Barral, J.M. (2005). De novo folding of GFP fusion proteins: High efficiency in eukaryotes but not in bacteria. J. Mol. Biol. *353*, 397–409.

Chun, S.Y., Strobel, S., Bassford, P., Jr., and Randall, L.L. (1993). Folding of maltose-binding protein. Evidence for the identity of the rate-determining step in vivo and in vitro. J. Biol. Chem. *268*, 20855–20862.

Ewalt, K.L., Hendrick, J.P., Houry, W.A., and Hartl, F.U. (1997). In vivo observation of polypeptide flux through the bacterial chaperonin system. Cell *90*, 491–500.

Fayet, O., Ziegelhoffer, T., and Georgopoulos, C. (1989). The GroES and GroEL heat shock gene products of Escherichia coli are essential for bacterial growth at all temperatures. J. Bacteriol. *171*, 1379–1385.

Fenton, W.A., Kashi, Y., Furtak, K., and Horwich, A.L. (1994). Residues in chaperonin GroEL required for polypeptide binding and release. Nature *371*, 614–619.

Fenton, W.A., and Horwich, A.L. (2003). Chaperonin-mediated protein folding: fate of substrate polypeptide. Q. Rev. Biophys. *36*, 229–256.

Ganesh, C., Zaidi, F.N., Udgaonkar, J.B., and Varadarajan, R. (2001). Reversible formation of on-pathway macroscopic aggregates during the folding of maltose binding protein. Prot. Sci. *10*, 1635–1644.

Guzman, L.M., Belin, D., Carson, M.J., and Beckwith, J. (1995). Tight regulation, modulation, and high-level expression by vectors containing the arabinose p-BAD promoter. J. Bacteriol. *177*, 4121–4130.

Hartl, F.U., and Hayer-Hartl, M. (2002). Molecular chaperones in the cytosol: from nascent chain to folded protein. Science *295*, 1852–1858.

Hayer-Hartl, M.K., Weber, F., and Hartl, F.U. (1996). Mechanism of chaperonin action: GroES binding and release can drive GroEL-mediated protein folding in the absence of ATP hydrolysis. EMBO J. *15*, 6111–6121.

Horst, R., Bertelsen, E.B., Fiaux, J., Wider, G., Horwich, A.L., and Wuthrich, K. (2005). Direct NMR observation of a substrate protein bound to the chaperonin GroEL. Proc. Natl. Acad. Sci. USA *102*, 12748–12753.

Horwich, A.L., Low, K.B., Fenton, W.A., Hirshfield, I.N., and Furtak, K. (1993). Folding in vivo of bacterial cytoplasmic proteins: role of GroEL. Cell *74*, 909–917.

Houry, W.A., Frishman, D., Eckerskorn, C., Lottspeich, F., and Hartl, F.U. (1999). Identification of in vivo substrates of the chaperonin GroEL. Nature *402*, 147–154.

Hunt, J.F., Vies, S.M., Henry, L., and Deisenhofer, J. (1997). Structural adaptations in the specialized bacteriophage T4 co-chaperonin Gp31 expand the size of the anfinsen cage. Cell *90*, 361–371.

Jewett, A.I., Baumketner, A., and Shea, J.E. (2004). Accelerated folding in the weak hydrophobic environment of a chaperonin cavity: Creation of an alternate fast folding pathway. Proc. Natl. Acad. Sci. USA *101*, 13192–13197.

Kerner, M.J., Naylor, D.J., Ishihama, Y., Maier, T., Chang, H.C., Stines, A.P., Georgopoulos, C., Frishman, D., Hayer-Hartl, M., Mann, M., and Hartl, F.U. (2005). Proteome-wide analysis of chaperonin-dependent protein folding in Escherichia coli. Cell *122*, 209–220.

Landry, S.J., Zeilstra, R.J., Fayet, O., Georgopoulos, C., and Gierasch, L.M. (1993). Characterization of a functionally important mobile domain of GroES. Nature *364*, 255–258.

Lin, Z., and Rye, H.S. (2004). Expansion and compression of a protein folding intermediate by GroEL. Mol. Cell *16*, 23–34.

Maisnier-Patin, S., Roth, J.R., Fredriksson, A., Nystrom, T., Berg, O.G., and Andersson, D.I. (2005). Genomic buffering mitigates the effects of deleterious mutations in bacteria. Nat. Genet. *37*, 1376–1379.

Marvin, J.S., Corcoran, E.E., Hattangadi, N.A., Zhang, J.V., Gere, S.A., and Hellinga, H.W. (1997). The rational design of allosteric interactions in a monomeric protein and its applications to the construction of biosensors. Proc. Natl. Acad. Sci. USA *94*, 4366–4371.

Mayhew, M., Da Silva, A.C.R., Martin, J., Erdjument-bromage, H., Tempst, P., and Hartl, F.U. (1996). Protein folding in the central cavity of the GroEL-GroES chaperonin complex. Nature *379*, 420–426.

McLennan, N.F., Girshovich, A.S., Lissin, N.M., Charters, Y., and Masters, M. (1993). The strongly conserved carboxyl-terminus glycine-methionine motif of the Escherichia coli GroEL chaperonin is dispensable. Mol. Microbiol. *7*, 49–58.

Ojha, A., Anand, M., Bhatt, A., Kremer, L., Jacobs, W.R., and Hatfull, G.F. (2005). GroEL1: A dedicated chaperone involved in mycolic acid biosynthesis during biofilm formation in mycobacteria. Cell *123*, 861–873.

Rutherford, S.L., and Lindquist, S. (1998). Hsp90 as a capacitor for morphological evolution. Nature *396*, 336–342.

Rye, H.S., Burston, S.G., Fenton, W.A., Beechem, J.M., Xu, Z., Sigler, P.B., and Horwich, A.L. (1997). Distinct actions of cis and trans ATP within the double ring of the chaperonin GroEL. Nature *388*, 792–798.

Saibil, H.R., and Ranson, N.A. (2002). The chaperonin folding machine. Trends Biochem. Sci. *27*, 627–632.

Sparrer, H., Rutkat, K., and Buchner, J. (1997). Catalysis of protein folding by symmetric chaperone complexes. Proc. Natl. Acad. Sci. USA *94*, 1096–1100.

Spurlino, J.C., Lu, G.Y., and Quiocho, F.A. (1991). The 2.3-Å resolution structure of the maltose- or maltodextrin-binding protein, a primary receptor of bacterial active transport and chemotaxis. J. Biol. Chem. *266*, 5202–5219.

Stan, G., Thirumalai, D., Lorimer, G.H., and Brooks, B.R. (2003). Annealing function of GroEL: structural and bioinformatic analysis. Biophys. Chem. *100*, 453–467.

Takagi, F., Koga, N., and Takada, S. (2003). How protein thermodynamics and folding mechanisms are altered by the chaperonin cage: Molecular simulations. Proc. Natl. Acad. Sci. USA *100*, 11367–11372.

Thirumalai, D., and Lorimer, G.H. (2001). Chaperonin-mediated protein folding. Annu. Rev. Biophys. Biomol. Struct. *30*, 245–269.

Vendruscolo, M., Paci, E., Karplus, M., and Dobson, C.M. (2003). Structures and relative free energies of partially folded states of proteins. Proc. Natl. Acad. Sci. USA *100*, 14817–14821.

Wang, J.D., Michelitsch, M.D., and Weissman, J.S. (1998). GroEL-GroES-mediated protein folding requires an intact central cavity. Proc. Natl. Acad. Sci. USA *95*, 12163–12168.

Wang, J.D., Herman, C., Tipton, K.A., Gross, C.A., and Weissman, J.S. (2002). Directed evolution of substrate-optimized GroEL/S chaperonins. Cell *111*, 1027–1039.

Weissman, J.S., Rye, H.S., Fenton, W.A., Beechem, J.M., and Horwich, A.L. (1996). Characterization of the active intermediate of a GroEL-GroES-mediated protein folding reaction. Cell *84*, 481–490.

Xu, Z.H., Horwich, A.L., and Sigler, P.B. (1997). The crystal structure of the asymmetric GroEL-GroES-(ADP)7 chaperonin complex. Nature *388*, 741–749.

Zhou, H.X. (2004). Protein folding and binding in confined spaces and in crowded solutions. J. Mol. Recognit. *17*, 368–375.